ACS OMEGA

http://pubs.acs.org/journal/acsodf

Article

Trace Compounds Confined in SAPO-34 and a Probable Evolution Route of Coke in the MTO Process

Mingjian Luo,* Bing Hu, Guoliang Mao, and Baohui Wang

Cite This: *ACS Omega* 2022, 7, 3277−3283

Read Online

ACCESS | Metrics & More | Article Recommendations | Supporting Information

ABSTRACT: Confined compounds in SAPO-34 cages are important to understand the activation and deactivation mechanisms of the methanol-to-olefin process. In this work, gas chromatography−mass spectrometry (GC-MS) chromatograms of CCl_4-extracted samples of used SAPO-34 were denoised by subtracting signals of air compounds and stationary phase bleeding of the chromatographic column, which enhanced the identification of trace compounds. In addition to the generally noted methyl aromatics, this work also identified alkanes, cycloalkanes, alkyl (ethyl, propyl, and butyl) compounds, partially saturated compounds, and bridged compounds. These novel identified trace compounds favor the evolution route depiction of monocyclic, bicyclic, tricyclic, tetracyclic, and multicore hydrocarbons in the SAPO-34 cage. Confined compounds should grow via step-by-step alkylation, cyclization, and aromatization processes. C_{2+} side chains, especially C_{3+}, favor the growth of rings. Alkyldihydroindenes should be key intermediates between monocyclic and bicyclic aromatics. Bridged soluble compounds provide evidence that insoluble coke is formed across cages in the SAPO-34 crystal.

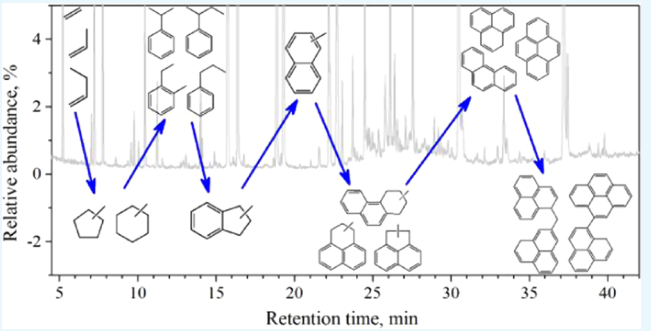

1. INTRODUCTION

Commercial methanol-to-olefin (MTO) plant with SAPO-34 zeolite as the catalyst was successfully constructed in China. This process provides a feasible non-petrochemical route to produce light olefins and chemicals. SAPO-34 zeolite provides moderate acidity that favors the formation of a carbocation intermediate. SAPO-34 also possesses a unique cage structure with highly connected small windows between cages, which provides a diffusion channel for methanol and light olefins as well as confines "hydrocarbon pool" compounds in cages. Therefore, SAPO-34 zeolite shows high methanol conversion activity and high olefin selectivity in the MTO process.

A SAPO-34-catalyzed MTO reaction involves three stages. The first stage is the coupling of methanol molecules on acidic sites to form the first C−C bond, which initiates the reaction. This early stage has been studied extensively. Indirect[1−3] and direct mechanisms[4−12] have been proposed. Recently, experimental results[11−14] and theoretical calculations[7,15,16] have demonstrated that the carbonylation mechanism is the most reasonable route to form the first C−C bond. The second stage is the highly efficient conversion of methanol under the cocatalyzation of acidic sites and confined organics. The reactions follow the "hydrocarbon pool" mechanism[3,8,17−22] in this stage. The third stage is the evolution of confined compounds from highly active "hydrocarbon pool" compounds to polycyclic aromatics.[23−29] These polycyclic aromatics block cages and lead to the deactivation of the catalyst. The key aspect in both the second and third stages is the type and amount of confined compounds. It was generally accepted that confined compounds in SAPO-34 cages were methyl aromatics with no more than four rings (pyrene).[19,29−32] Methylbenzenes and methylnaphthalenes act as "hydrocarbon pool" compounds and promote the conversion of methanol. Three- and four-ring compounds block the diffusion channel and lead to deactivation. Small cyclic compounds like tetramethylcyclohexane,[33] adamantane,[33−35] and methylcyclopentadienes[36,37] were also identified. Recently, it has been found that even larger aromatics located across cage windows can also be formed.[23−25] Based on these identified compounds, some preliminary mechanisms on the evolution route of confined compounds were supposed. For example, Konnov et al.[24] supposed that olefins participated in the growth of rings. Dai et al.[27] supposed that the formation of large alkyl chain aromatics is the most important step of deactivation. Very recently, Yu et al.[38] identified the presence of tetrahydro-1,8-dimethylnaphthalene, dihydro-1,5,6-trimethyl-1*H*-indene, and 1,2-dimethyl-3-(2-butenyl)benzene. These intermediates make the transformation from methylbenzenes to methylnaphthalene clear.

Received: September 26, 2021
Accepted: January 12, 2022
Published: January 20, 2022

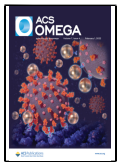

https://doi.org/10.1021/acsomega.1c05336
ACS Omega 2022, 7, 3277−3283

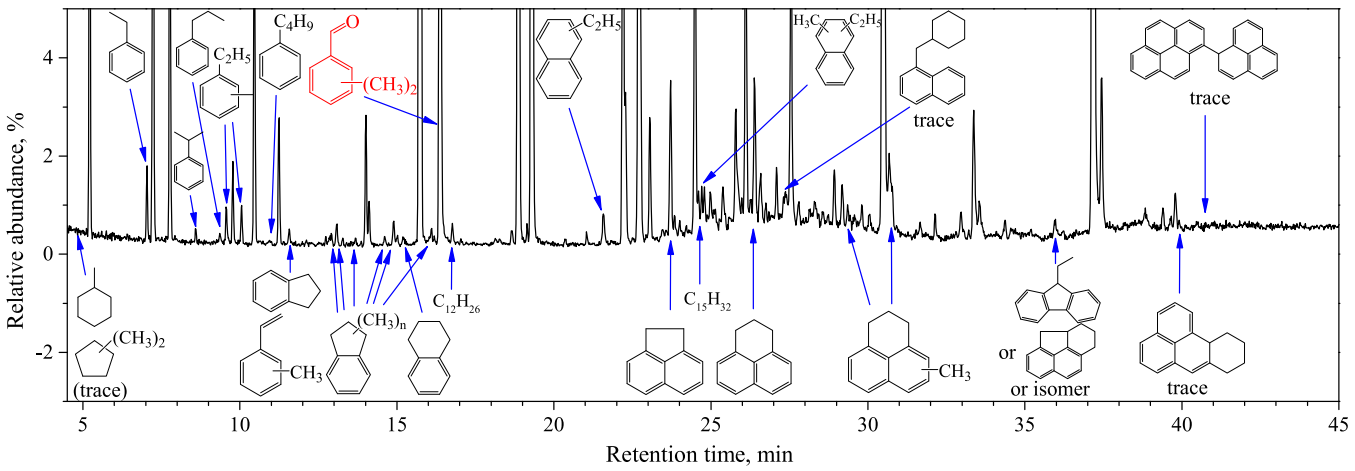

Figure 1. GC-MS total ion chromatogram and identified confined compounds other than the methyl aromatics from a methanol feed.

However, large alkyl chain aromatics have not been detected in the SAPO-34-catalyzed process yet. Intermediates between aromatics with 1, 2, 3, 4, and an even larger number of rings are still unclear.

Confined compounds in SAPO-34 cages have been extensively studied by GC-MS analysis of the extraction phase of the dissolved coked catalyst.[25,29−40] However, background signals from air components and stationary phase bleeding of the chromatographic column are unavoidable. They overlapped with signals of compounds, which renders the signals of trace compounds obscure or even unobservable. In this work, GC-MS spectra of extracted confined compounds were denoised. Trace compounds other than the generally noted methyl aromatics were identified. Based on these trace compounds, the evolution route of confined compounds in SAPO-34 cages was discussed.

2. RESULTS

Figure 1 shows the GC-MS total ion chromatogram and identified confined compounds other than generally noted methyl aromatics from a methanol feed. More detailed results are shown in Table S1 and Figures S2−S5. In addition to methyl aromatics, this work identified alkanes, cycloalkanes, alkyl (ethyl, propyl, butyl) compounds, partially saturated compounds (2,3-dihydro-1*H*-indene, 1,2,3,4-tetrahydronaphthalene, 2,3-dihydro-1*H*-phenalene, etc.), and bridged compounds in all samples.

2.1. Alkanes. The first type of the newly identified confined compound is C_{12-19} alkanes (Nos. **62**, **71**, **75**, **91**, **110**, **118**, **130**, etc., Table S1). Figures 2A and S6 show typical fragment ion spectra of these alkanes. Olefin feeds tend to form more alkanes than methanol feeds. For example, relative abundances of dodecane (No. **62**) were 2.05, 1.45, 5.54, and 0.42 for 1-butene, propene, ethene, and methanol feeds, respectively. Therefore, large alkanes should be formed via the addition reactions between olefins[41] and the following hydrogen transfer. Considering that long alkanes are easy to crack on acidic sites at the reaction temperature (425 °C), these large alkanes should be formed in cages with weak or no acidic sites. Alkanes with less than 12 carbon atoms (C_{12-}) and more than 20 carbon atoms (C_{20+}) were not observed. The absence of C_{12-} alkanes can be ascribed to their relatively small size. They diffuse into adjacent cages with acidic sites and then crack or cyclize. The C_{20+} alkanes are too large to be formed in a cage, and thus they were not detected as well.

2.2. Cycloalkanes. The second type of novel identified confined compounds is C_5−C_8 cycloalkanes (Nos. **1**−**4**, **6**−**8**, Figure 2B, Table S1 and Figure S7). They were also detected in the product of the ZSM-5-catalyzed methanol conversion process.[42] Cycloalkanes exhibited very low relative abundances. Even for the 1-butene feed, which tends to generate more cycloalkanes than other feeds, the relative abundances of cycloalkanes were in the range of 0.07−0.31%.

2.3. Alkylaromatics. The presence and role of methylbenzenes in the MTO process have been focused on for a long time. Methylbenzenes are found to be high-efficiency "hydrocarbon pool" compounds in the MTO process.[1,8,17−20,32,43,44] Methylnaphthalenes are found to be about one-third as active as methylbenzenes and tend to obtain higher ethene selectivity than methylbenzenes.[45] However, C_{2+} alkyl (ethyl, propyl, etc.) aromatics were not be identified before the very recent work of Yu et al.[38] In their work, Yu et al. reported the identification of 1,2-dimethyl-3-(2-butenyl)benzene and regarded this compound to be one of the key coke precursors.

In this work, ethyl, propyl, isopropyl, butyl, and isobutylbenzene were detected (Nos. **9**, **12**, **14**−**16**, **20**−**24**, **26**−**29**, **34**, **37**, **39**, **42**, etc., Figure 2C, Table S1 and Figure S8). It was found that the formation of alkylbenzenes is related to feeds. As shown in Table S1, the relative abundance of ethylbenzene was 14.6% for the ethene feed, while the values for 1-butene, propene, and methanol feeds were 1.8, 0.7, and 1.6%, respectively, which implied that ethene is much more active to form ethylbenzene than other feeds. Similarly, propene and 1-butene favor the formation of compounds containing isopropyl and isobutyl, respectively. Moreover, the relative abundances of C_{2+} side-chain compounds were considerably high. For example, the sum of relative abundances of isopropylbenzene (No. **12**), propylbenzene (No. **14**), and ethylmethylbenzene (Nos. **15** and **16**) were 4.2, 3.1, 9.9, and 1.9% for 1-butene, propene, ethene, and methanol feeds, respectively. The values of trimethylbenzenes (Nos. **17**−**19**) were 10.7, 3.0, 6.3, and 12.1%, respectively. The abundance of C_{2+} side-chain benzenes was similar to or of the same order of magnitude as generally noted methylbenzenes. Relative abundances of C_{2+} side-chain benzenes indicate that the alkylation of benzene with olefin is non-negligible in the reaction network.

https://doi.org/10.1021/acsomega.1c05336
ACS Omega 2022, 7, 3277−3283

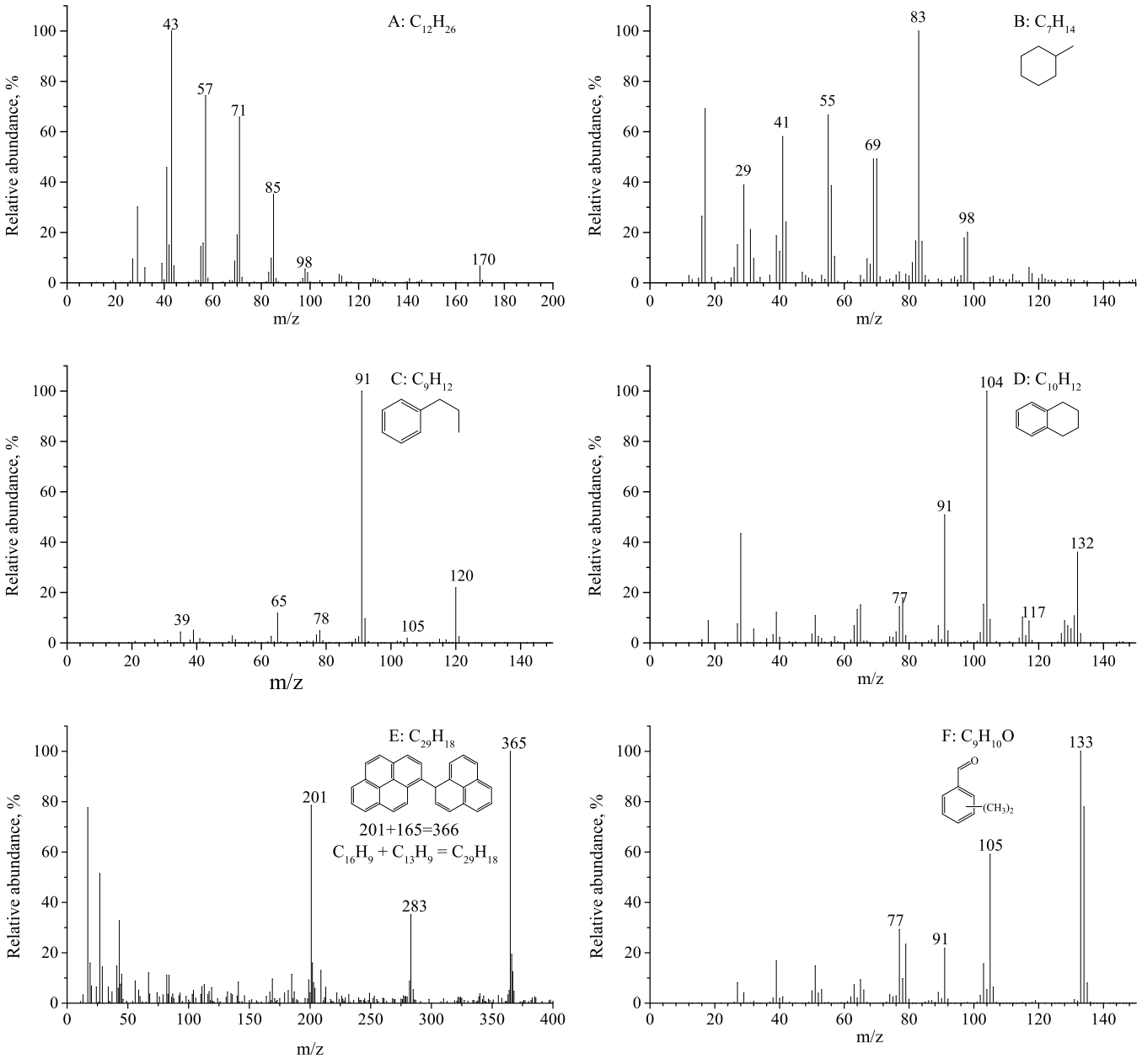

Figure 2. Fragment ion spectra of typical novel identified confined alkane (A: $C_{12}H_{26}$, No. **62**), cycloalkane (B: C_7H_{14}, No. **3**), alkylaromatic compound (C: C_9H_{12}, No. **14**), partially saturated bicyclic compound (D: $C_{10}H_{12}$, No. **53**), bridged compound (E: $C_{29}H_{18}$, No. **140**), and dimethylbenzaldehyde (F: $C_9H_{10}O$, No. **60**). Numbers are derived from Table S1.

C_{2+} side-chain naphthalenes were also detected (Nos. **80**, **85**, **89**, **92**−**93**, **96**−**98**, **104**−**105**, **109**, **111**, **113**, etc., Table S1). However, C_3 and C_4 side-chain naphthalenes were hardly detected in samples of methanol and ethene feeds.

2.4. Partially Saturated Bi-, Tri-, and Tetracyclic Compounds. Partially saturated bicyclic (Nos. **25**, **32**−**33**, **35**−**36**, **49**, **51**, **53**, **56**−**58**, **64**, **67**, **77**, **84**, etc., Figure 2D, Table S1 and Figure S9), tricyclic (Nos. **79**, **86**−**88**, **99**, **103**, **107**, **114**, etc.), and tetracyclic (Nos. **129**, **132**, **138**, etc.) compounds, which are precursors of bi-, tri-, and tetracyclic aromatics, were identified as well. They exhibited much higher abundances than cyclopentane, cyclohexane, and their alkylated products. For example, the relative abundances of 2,3-dihydro-1*H*-indene (No. **25**) were 1.3, 0.27, 1.8, and 0.31% for 1-butene, propene, ethene, and methanol feeds, respectively. Values of methyl-2,3-dihydro-1*H*-indene (Nos. **32**−**33**) were 2.9, 0.88, 3.2, and 0.68%, respectively. Values of 1,2,3,4-tetrahydronaphthalene (No. **53**) were 1.5, 0.54, 1.5, and 0.17%, respectively. Partially saturated tri- and tetracyclic compounds exhibited relatively high abundances in olefin feed products, while hardly observable abundance in the methanol feed product.

2.5. Bridged Compounds and Molecules Larger Than the SAPO-34 Cage Size. Another type of novel identified compounds is bridged compounds (Nos. **78**, **106**, **108**, **139**−**141**, Figure 2E, Table S1 and Figure S10). Biphenyl (No. **78**) and methylbiphenyls (Nos. **106** and **108**) exhibited relatively high abundances in samples from methanol and ethene feeds. Cyclohexylmethylnaphthalene (No. **139**), phenalen-1-yl-pyrene (No. **140**), and methylene bisphenalene (No. **141**), especially the latter two, were present in trace amounts in all samples. The peaks were obscure in the total ion chromato-

https://doi.org/10.1021/acsomega.1c05336
ACS Omega 2022, 7, 3277−3283

Scheme 1. Proposed Evolution Route of Confined Compounds in SAPO-34[a]

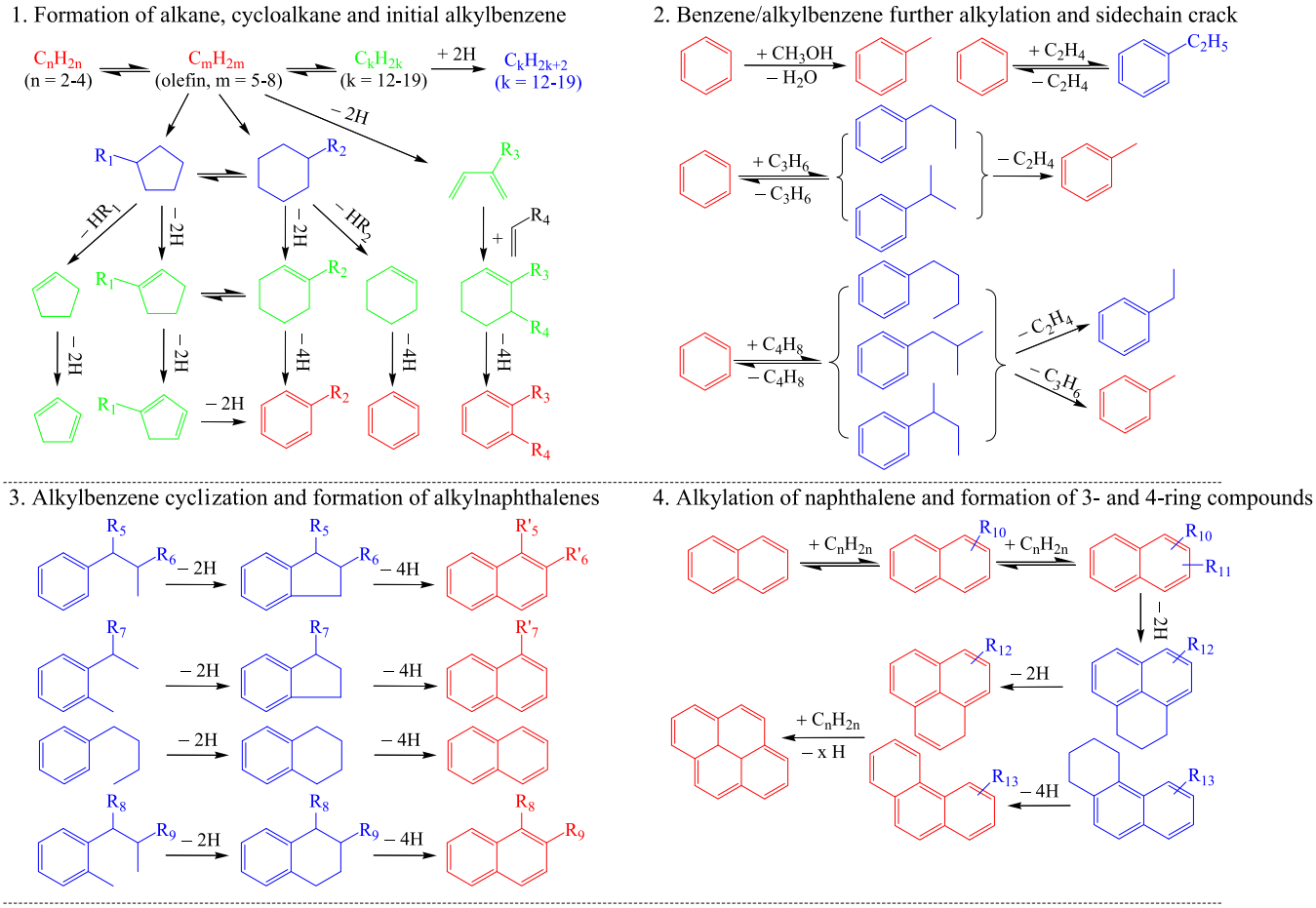

[a]Red: commonly noted confined compounds or products; blue: novel identified confined compounds; green: probable intermediates; +H and −H: hydrogen transfer; $R_{1-9,12-13}$: H, CH_3, ...; R_{10-11}: CH_3, C_2H_5, C_3H_7, ...; in ring-expanding reactions, $R_1 = R_2 + CH_2$; $R_5 = R'_5 + CH_2$, or $R_6 = R'_6 + CH_2$; $R_7 = R'_7 + CH_2$.

gram. However, as shown in Figure S10F, very clear peaks were observed at 44.4 min (No. **140**) on chromatogram of ions with m/z values of 201, 283, and 365 and at 45.4 min (No. **141**) on chromatogram of ions with m/z values of 179, 261, and 343.

2.6. Dimethylbenzaldehyde. Dimethylbenzaldehyde (No. **60**, Figure 2F), which has the same molelecular ion (m/z value of 134) as tetramethylbenzene, is found in high abundance in samples from methanol while absent in samples from ethene, propene, and 1-butene. Many studies[3−7] showed a high content of tetramethylbenzene. However, compound **60** should not be tetramethylbenzene since tetramethylbenzenes exhibit a high intensity at an m/z of 119, while this compound shows a very weak signal at an m/z of 119. The fragment ion spectrum of this compound is well consistent with that of dimethylbenzaldehyde. Its formation mechanism and its role in the MTO reaction need further study.

3. DISCUSSION

Many studies have discussed the formation and the role of "hydrocarbon pool" and coke compounds in the SAPO-34-catalyzed MTO process.[3,21,28,29,46] The evolution of confined compounds has been agreed to be a step-by-step ring growth

https://doi.org/10.1021/acsomega.1c05336
ACS Omega 2022, 7, 3277−3283

process. However, intermediates between aromatics are still unclear.

The novel detected low content or even trace abundance compounds are important intermediates for the formation of olefins and the evolution of confined compounds. Based on these compounds, an evolution route of confined compounds is proposed in Scheme 1.

The formation of confined compounds should begin with the oligomerization and alkylation of light olefins, which lead to the formation of large olefins. The oligomerization and alkylation of olefins are inevitable in acidic site-catalyzed hydrocarbon conversion processes.[3,47,48] However, no confined olefins were detected in SAPO-34 cages. This can be attributed to the fact that light olefins tend to diffuse out from the SAPO-34 crystal, while the C_{6+}, due to their high reactivity, crack to form light ones, hydrogen transfer to form alkanes, or cyclize to form cycloalkanes. These light alkanes, such as methane, ethane, etc., are byproducts of the MTO process. Heavy alkanes (C_{12}−C_{19}), which have low diffusivity, are trapped in SAPO-34 cages and detected in the dissolution-extraction phase.

Cycloalkanes should be formed via the cyclization of C_{5+} olefins.[49,50] Many studies have also detected cyclopentyl, cyclopentenyl, and cyclopentadienyl with NMR spectra.[36,37,51] These five-membered cyclic compounds were supposed to be active "hydrocarbon pool" species, and they were further transferred into methylbenzenes. Cycloalkanes were identified in this work, which supports the supposition that cycloalkanes are precursors of methylbenzenes. However, cyclenes and cyclic dienes were not detected in the extraction phase. It can be attributed to the fact that cyclenes and cyclic dienes have high activity to undergo the hydrogen transfer reaction to form alkylbenzenes.

Initial alkylbenzenes should be formed via the dehydrogenation of cycloalkanes[49,50] or the dehydrogenation of Diels−Alder products.[52,53] Then, these alkylbenzenes alkylate with olefins or methanol. Methanol, ethene, propene, and butene favor the formation of methyl, ethyl, isopropyl, and isobutyl, respectively (Table S1). Alkylbenzenes undergo further pairing and side-chain cracking reactions, which affect product selectivity of the MTO process. Alkylbenzenes also further undergo cyclization to form bicyclic compounds.

The further cyclization and dehydrogenation of alkylbenzenes lead to the formation of partially saturated bicyclic compounds, followed by naphthalene, tricyclic, and tetracyclic compounds. To form alkyltetrahydronaphthalenes, the precursor alkylbenzenes should have a four-carbon length side chain (e.g., No. **20**) or a three-carbon length side chain and an adjacent methyl (Nos. **29**, **39**, etc.). However, the abundances of these precursors were very low (Table S1). The sample from the 1-butene feed was the only one that showed relatively high abundances of tetrahydronaphthalenes. Similarly, a precursor of alkyldihydroindenes requires a three-carbon length side chain (Nos. **14**, **21**, **29**, etc.) or ethyl with adjacent methyl (Nos. **15**, **16**, **22**−**24**, etc.). There were many of these precursors. As a result, alkyldihydroindenes have much more types and exhibit much higher abundances than alkyltetrahydronaphthalenes. Therefore, alkyldihydroindenes should be key intermediates between monocyclic and bicyclic aromatics. The supposition is consistent with that proposed by Yu et al.[38]

Alkyldihydroindenes undergo hydrogen transfer and ring expansion to form naphthalene and alkylnaphthalenes. The further alkylation−cyclization−hydrogen transfer of bicyclic compounds leads to the formation of tri- and tetracyclic compounds. The identified C_{2+} side-chain naphthalenes (Nos. **80**, **85**, **89**, **92**−**93**, **96**−**98**, **104**−**105**, **109**, **111**, **113**, etc.) and partially saturated tri- and tetracyclic compounds (Nos. **79**, **86**−**88**, **99**, **103**, **107**, **114**, **129**, **132**, **138**, etc.) are intermediates between bi-, tri-, and tetracyclic aromatics.

As discussed above, the evolution route of mono-, bi-, tri-, and tetracyclic compounds is a step-by-step process. This process is composed of alkylation, cyclization, and aromatization (hydrogen transfer). The novel detected alkanes, cycloalkanes, alkyl compounds, and partially saturated compounds bridge the gap between aromatics with 1, 2, 3, 4, and an even larger number of rings, which makes the evolution route of confined compounds more complete. Additionally, cyclization is the key step of ring growth. This step involves long-chain olefin or long side-chain alkyl. 1-Butene and propene exhibit a much higher reactivity and tend to form longer side-chain alkyl. Thus, 1-butene and propene showed much higher coking rates than ethene.[39,40]

Bridged compounds (Nos. **78**, **106**, **108**, **139**−**141**) might be formed via step-by-step growth or the direct bridging mechanism within adjacent cages (Scheme 1). The adjacent cages share the conjunct eight-member window, which makes the alkylation across the cage window feasible. Then, bridged compounds are formed via step-by-step cyclization and hydrogen transfer. Additionally, three- and four-ring species are similar in size to the cage. If they are formed in adjacent cages, they should be close enough to link directly, which leads to the formation of bridged compounds like **140** and **141**, too. These bridged structures should be a precursor of recently noted insoluble coke. Temperature programming MS[39,54] and matrix-assisted laser desorption/ionization time-of-flight mass spectrometry (MALDI-TOF MS)[23,24] results of insoluble coke showed a periodic m/z group distribution with an interval of 160−200, just the mass of three- and four-ring aromatics. The novel identified bridged compounds are also composed of three- and four-ring aromatics. Structures of bridged compounds provide evidence for interpreting the structure of insoluble coke.

4. CONCLUSIONS

Alkanes, cycloalkanes, alkyl (ethyl, propyl, butyl) compounds, partially saturated compounds, and bridged compounds were identified in SAPO-34 cages. These novel identified trace compounds are intermediates between aromatics with 1, 2, 3, 4, and an even larger number of rings. They favor the depiction of the evolution route of monocyclic, bicyclic, tricyclic, tetracyclic, and multicore hydrocarbons in the SAPO-34 cage. Confined compounds grow via step-by-step alkylation, cyclization, and aromatization process. C_{2+} side chains, especially C_{3+}, favor the growth of rings. Alkyldihydroindenes are key intermediates between monocyclic and bicyclic aromatics. Bridged soluble compounds provide evidence that insoluble coke can be formed across cages in the SAPO-34 crystal.

5. EXPERIMENTS

Properties of SAPO-34 and experimental details were described in our previous work.[25,39] Reactions were performed at atmosphere pressure and 425 °C with methanol (WHSV = 1 h^{-1}) or olefin (1-butene, propene, or ethene, WHSV = 0.5 h^{-1}) feeds for 200 min. Coke weights were 192.5, 79.7, 70.8, and 6.2

https://doi.org/10.1021/acsomega.1c05336
ACS Omega 2022, 7, 3277−3283

mg_{coke}/g_{cat} for methanol, 1-butene, propene, and ethene feeds, respectively. Coked SAPO-34 (15 mg) was dissolved in 0.5 mL of 10% HF, extracted with 150 μL of CCl_4, and then the CCl_4 phase was analyzed on a Thermo Fisher Trace GC-MS equipped with a TR-1 MS capillary column (30 m × 0.25 mm × 0.25 μm). Mass spectra were recorded in an m/z range of 15−500. Relative abundance was based on naphthalene, which exhibited the highest abundance (100% abundance).

Unavoidable trace leakage air and column bleeding signals were subtracted from the original total ion chromatogram to obtain the denoised one. The m/z values of 18, 28, 32, 40, and 44, which mainly or partially relate to signals of H_2O, N_2, O_2, Ar, and CO_2, were regarded as air signals. The m/z values of 73, 147, 167, 207, 256, 267, 281, etc., mainly or partially correspond to signals of column bleeding. Comparison of the original and denoised GC-MS chromatograms of the extracted phase from the methanol feed is shown in Figure S1. Obviously, many indefinite peaks became identifiable in the denoised chromatogram. The identification of confined compounds was mainly based on the matching results of fragment ion spectra with the NIST MS database. However, due to the presence of isomers, the overlapping of peaks, the noise of signals, the low content, and the limitation of the NIST database, some peaks cannot be well matched. Structures of these peaks were deduced with consideration of feed and reaction characteristics. Details of typical peaks are discussed in the Supporting Information.

■ ASSOCIATED CONTENT

Supporting Information

The Supporting Information is available free of charge at https://pubs.acs.org/doi/10.1021/acsomega.1c05336.

Experimental details, confined compounds, GC-MS total ion chromatograms, typical fragment ion spectra, and deduction of typical compounds (PDF)

■ AUTHOR INFORMATION

Corresponding Author

Mingjian Luo − *Provincial Key Laboratory of Oil & Gas Chemical Technology, College of Chemistry & Chemical Engineering, Northeast Petroleum University, Daqing 163318 Heilongjiang, P. R. China;* orcid.org/0000-0001-8199-0269; Email: luomingjian@nepu.edu.cn

Authors

Bing Hu − *Provincial Key Laboratory of Oil & Gas Chemical Technology, College of Chemistry & Chemical Engineering, Northeast Petroleum University, Daqing 163318 Heilongjiang, P. R. China*

Guoliang Mao − *Provincial Key Laboratory of Oil & Gas Chemical Technology, College of Chemistry & Chemical Engineering, Northeast Petroleum University, Daqing 163318 Heilongjiang, P. R. China*

Baohui Wang − *Provincial Key Laboratory of Oil & Gas Chemical Technology, College of Chemistry & Chemical Engineering, Northeast Petroleum University, Daqing 163318 Heilongjiang, P. R. China;* orcid.org/0000-0003-2547-9954

Complete contact information is available at: https://pubs.acs.org/10.1021/acsomega.1c05336

Notes

The authors declare no competing financial interest.

■ ACKNOWLEDGMENTS

The authors thank the Natural Science Foundation of Heilongjiang Provincial (LH2020B002) and NEPU Cultivate Science Foundation (2019YDL-13) for financial support.

■ REFERENCES

(1) Haw, J. F.; Song, W.; Marcus, D. M.; Nicholas, J. B. The mechanism of methanol to hydrocarbon catalysis. *Acc. Chem. Res.* **2003**, *36*, 317−326.

(2) Vogt, C.; Weckhuysen, B. M.; Ruiz-Martínez, J. Effect of feedstock and catalyst impurities on the methanol-to-olefin Reaction over H-SAPO-34. *ChemCatChem* **2017**, *9*, 183−194.

(3) Yarulina, I.; Chowdhury, A. D.; Meirer, F.; Weckhuysen, B. M.; Gascon, J. Recent trends and fundamental insights in the methanol-to-hydrocarbons process. *Nat. Catal.* **2018**, *1*, 398−411.

(4) Wu, X.; Xu, S.; Zhang, W.; Huang, J.; Li, J.; Yu, B.; Wei, Y.; Liu, Z. Direct mechanism of the first carbon−carbon bond formation in the methanol-to-hydrocarbons process. *Angew. Chem., Int. Ed.* **2017**, *56*, 9039−9043.

(5) Peng, C.; Wang, H.; Hu, P. Theoretical insights into how the first C-C bond forms in the methanol-to-olefin process catalysed by HSAPO-34. *Phys. Chem. Chem. Phys.* **2016**, *18*, 14495−14502.

(6) Lercher, J. A. New lewis acid catalyzed pathway to carbon−carbon bonds from methanol. *ACS Cent. Sci.* **2015**, *1*, 350−351.

(7) Plessow, P. N.; Studt, F. Unraveling the mechanism of the initiation reaction of the methanol to olefins process using ab initio and DFT calculations. *ACS Catal.* **2017**, *7*, 7987−7994.

(8) Dai, W.; Wang, C.; Dyballa, M.; Wu, G.; Guan, N.; Li, L.; Xie, Z.; Hunger, M. Understanding the early stages of the methanol-to-olefin conversion on H-SAPO-34. *ACS Catal.* **2015**, *5*, 317−326.

(9) Li, J.; Wei, Z.; Chen, Y.; Jing, B.; He, Y.; Dong, M.; Jiao, H.; Li, X.; Qin, Z.; Wang, J.; Fan, W. A route to form initial hydrocarbon pool species in methanol conversion to olefins over zeolites. *J. Catal.* **2014**, *317*, 277−283.

(10) Yamazaki, H.; Shima, H.; Imai, H.; Yokoi, T.; Tatsumi, T.; Kondo, J. N. Evidence for a "Carbene-like" Intermediate during the Reaction of Methoxy Species with Light Alkenes on H-ZSM-5. *Angew. Chem., Int. Ed.* **2011**, *50*, 1853−1856.

(11) Comas-Vives, A.; Valla, M.; Copéret, C.; Sautet, P. Cooperativity between Al Sites Promotes Hydrogen Transfer and Carbon−Carbon Bond Formation upon Dimethyl Ether Activation on Alumina. *ACS Cent. Sci.* **2015**, *1*, 313−319.

(12) Liu, Y.; Müller, S.; Berger, D.; Jelic, J.; Reuter, K.; Tonigold, M.; Sanchez-Sanchez, M.; Lercher, J. A. Formation mechanism of the first carbon−carbon bond and the first olefin in the methanol conversion into hydrocarbons. *Angew. Chem., Int. Ed.* **2016**, *55*, 5723−5726.

(13) Chowdhury, A. D.; Houben, K.; Whiting, G. T.; Mokhtar, M.; Asiri, A. M.; Al-Thabaiti, S. A.; Basahel, S. N.; Baldus, M.; Weckhuysen, B. M. Initial carbon−carbon bond formation during the early stages of the methanol-to-olefin process proven by zeolite-trapped acetate and methyl acetate. *Angew. Chem., Int. Ed.* **2016**, *55*, 15840−15845.

(14) Chen, Z.; Ni, Y.; Zhi, Y.; Wen, F.; Zhou, Z.; Wei, Y.; Zhu, W.; Liu, Z. Coupling of Methanol and Carbon Monoxide over H-ZSM-5 to Form Aromatics. *Angew. Chem., Int. Ed.* **2018**, *57*, 12549−12553.

(15) Plessow, P. N.; Studt, F. Theoretical Insights into the Effect of the Framework on the Initiation Mechanism of the MTO Process. *Catal. Lett.* **2018**, *148*, 1246−1253.

(16) Zang, K.; Zhang, W.; Huang, J.; Feng, P.; Ding, J. First molecule with carbon−carbon bond in methanol-to-olefins process. *Chem. Phys. Lett.* **2019**, *737*, No. 136844.

(17) Dahl, I. M.; Kolboe, S. On the reaction mechanism for propene formation in the MTO reaction over SAPO-34. *Catal. Lett.* **1993**, *20*, 329−336.

(18) Dahl, I. M.; Kolboe, S. On the reaction mechanism for hydrocarbon formation from methanol over SAPO-34. I. Isotopic labeling studies of the co-reaction of ethene and methanol. *J. Catal.* **1994**, *149*, 458−464.
(19) Wei, Y.; Zhang, D.; Chang, F.; Xia, Q.; Su, B.-l.; Liu, Z. Ultra-short contact time conversion of chloromethane to olefins over pre-coked SAPO-34: direct insight into the primary conversion with coke deposition. *Chem. Commun.* **2009**, 5999−6001.
(20) Qian, Q.; Vogt, C.; Mokhtar, M.; Asiri, A. M.; Al-Thabaiti, S. A.; Basahel, S. N.; Ruiz-Martínez, J.; Weckhuysen, B. M. Combined operando UV/Vis/IR spectroscopy reveals the role of methoxy and aromatic species during the methanol-to-olefins reaction over H-SAPO-34. *ChemCatChem* **2014**, *6*, 3396−3408.
(21) Ilias, S.; Bhan, A. Mechanism of the catalytic conversion of methanol to hydrocarbons. *ACS Catal.* **2013**, *3*, 18−31.
(22) Yang, M.; Fan, D.; Wei, Y.; Tian, P.; Liu, Z. Recent progress in methanol-to-olefins (MTO) catalysts. *Adv. Mater.* **2019**, *31*, No. 1902181.
(23) Wang, N.; Zhi, Y.; Wei, Y.; Zhang, W.; Liu, Z.; Huang, J.; Sun, T.; Xu, S.; Lin, S.; He, Y.; Zheng, A.; Liu, Z. Molecular elucidating of an unusual growth mechanism for polycyclic aromatic hydrocarbons in confined space. *Nat. Commun.* **2020**, *11*, No. 1079.
(24) Konnov, S. V.; Pavlov, V. S.; Kots, P. A.; Zaytsev, V. B.; Ivanova, I. I. Mechanism of SAPO-34 catalyst deactivation in the course of MTO conversion in a slurry reactor. *Catal. Sci. Technol.* **2018**, *8*, 1564−1577.
(25) Luo, M.; Zang, H.; Hu, B.; Wang, B.; Mao, G. Evolution of confined species and their effects on catalyst deactivation and olefin selectivity in SAPO-34 catalyzed MTO process. *RSC Adv.* **2016**, *6*, 17651−17658.
(26) Rojo-Gama, D.; Etemadi, S.; Kirby, E.; Lillerud, K. P.; Beato, P.; Svelle, S.; Olsbye, U. Time- and space-resolved study of the methanol to hydrocarbons (MTH) reaction - influence of zeolite topology on axial deactivation patterns. *Faraday Discuss.* **2017**, *197*, 421−446.
(27) Dai, W.; Wu, G.; Li, L.; Guan, N.; Hunger, M. Mechanisms of the deactivation of SAPO-34 materials with different crystal sizes applied as MTO catalysts. *ACS Catal.* **2013**, *3*, 588−596.
(28) Chen, D.; Moljord, K.; Holmen, A. A methanol to olefins review: diffusion, coke formation and deactivation on SAPO type catalysts. *Microporous Mesoporous Mater.* **2012**, *164*, 239−250.
(29) Olsbye, U.; Svelle, S.; Lillerud, K. P.; Wei, Z. H.; Chen, Y. Y.; Li, J. F.; Wang, J. G.; Fan, W. B. The formation and degradation of active species during methanol conversion over protonated zeotype catalysts. *Chem. Soc. Rev.* **2015**, *44*, 7155−7176.
(30) Ying, L.; Ye, M.; Cheng, Y. W.; Li, X. Characteristics of Coke Deposition Over a SAPO-34 Catalyst in the Methanol-to-Olefins Reaction. *Pet. Sci. Technol.* **2015**, *33*, 984−991.
(31) Rostami, R. B.; Ghavipour, M.; Di, Z.; Wang, Y.; Behbahani, R. M. Study of coke deposition phenomena on the SAPO_34 catalyst and its effects on light olefin selectivity during the methanol to olefin reaction. *RSC Adv.* **2015**, *5*, 81965−81980.
(32) Arstad, B.; Kolboe, S. Methanol-to-hydrocarbons reaction over SAPO-34. Molecules confined in the catalyst cavities at short time on stream. *Catal. Lett.* **2001**, *71*, 209−212.
(33) Wei, Y.; Yuan, C.; Li, J.; Xu, S.; Zhou, Y.; Chen, J.; Wang, Q.; Xu, L.; Qi, Y.; Zhang, Q.; Liu, Z. Coke formation and carbon atom economy of methanol-to-olefins reaction. *ChemSusChem* **2012**, *5*, 906−912.
(34) Wei, Y.; Li, J.; Yuan, C.; Xu, S.; Zhou, Y.; Chen, J.; Wang, Q.; Zhang, Q.; Liu, Z. Generation of diamondoid hydrocarbons as confined compounds in SAPO-34 catalyst in the conversion of methanol. *Chem. Commun.* **2012**, *48*, 3082−3084.
(35) Yuan, C.; Wei, Y.; Li, J.; Xu, S.; Chen, J.; Zhou, Y.; Wang, Q.; Xu, L.; Liu, Z. Temperature-Programmed Methanol Conversion and Coke Deposition on Fluidized-Bed Catalyst of SAPO-34. *Chin. J. Catal.* **2012**, *33*, 367−374.
(36) Zhang, W.; Zhang, M.; Xu, S.; Gao, S.; Wei, Y.; Liu, Z. Methylcyclopentenyl Cations Linking Initial Stage and Highly Efficient Stage in Methanol-to-Hydrocarbon Process. *ACS Catal.* **2020**, 4510−4516.
(37) Zhang, W.; Zhi, Y.; Huang, J.; Wu, X.; Zeng, S.; Xu, S.; Zheng, A.; Wei, Y.; Liu, Z. Methanol to olefins reaction route based on methylcyclopentadienes as critical intermediates. *ACS Catal.* **2019**, *9*, 7373−7379.
(38) Yu, B.; Zhang, W.; Wei, Y.; Wu, X.; Sun, T.; Fan, B.; Xu, S.; Liu, Z. Capture and identification of coke precursors to elucidate the deactivation route of the methanol-to-olefin process over H-SAPO-34. *Chem. Commun.* **2020**, *56*, 8063−8066.
(39) Hu, B.; Mao, G.; Wang, D.; Fu, Y.; Wang, B.; Luo, M. Conversion and coking of olefins on SAPO-34. *Catal. Sci. Technol.* **2017**, *7*, 5785−5794.
(40) Zhou, J.; Zhi, Y.; Zhang, J.; Liu, Z.; Zhang, T.; He, Y.; Zheng, A.; Ye, M.; Wei, Y.; Liu, Z. Presituated "coke"-determined mechanistic route for ethene formation in the methanol-to-olefins process on SAPO-34 catalyst. *J. Catal.* **2019**, *377*, 153−162.
(41) Guisnet, M.; Magnoux, P. Organic chemistry of coke formation. *Appl. Catal., A* **2001**, *212*, 83−96.
(42) Schulz, H. "Coking" of zeolites during methanol conversion: Basic reactions of the MTO-, MTP- and MTG processes. *Catal. Today* **2010**, *154*, 183−194.
(43) Olsbye, U.; Bjørgen, M.; Svelle, S.; Lillerud, K. P.; Kolboe, S. Mechanistic insight into the methanol-to-hydrocarbons reaction. *Catal. Today* **2005**, *106*, 108−111.
(44) Wang, C.-M.; Wang, Y.-D.; Liu, H.-X.; Xie, Z.-K.; Liu, Z.-P. Catalytic activity and selectivity of methylbenzenes in HSAPO-34 catalyst for the methanol-to-olefins conversion from first principles. *J. Catal.* **2010**, *271*, 386−391.
(45) Song, W.; Fu, H.; Haw, J. F. Selective synthesis of methylnaphthalenes in HSAPO-34 cages and their function as reaction centers in methanol-to-olefin catalysis. *J. Phys. Chem. B* **2001**, *105*, 12839−12843.
(46) Xu, S.; Zhi, Y.; Han, J.; Zhang, W.; Wu, X.; Sun, T.; Wei, Y.; Liu, Z. Chapter Two - Advances in Catalysis for Methanol-to-Olefins Conversion. In *Advances in Catalysis*; Song, C., Ed.; Academic Press, 2017; Vol. *61*, pp 37−122.
(47) Ghashghaee, M. Heterogeneous catalysts for gas-phase conversion of ethylene to higher olefins. *Rev. Chem. Eng.* **2018**, *34*, 595−655.
(48) Vandichel, M.; Lesthaeghe, D.; Van der Mynsbrugge, J.; Waroquier, M.; Van Speybroeck, V. Assembly of cyclic hydrocarbons from ethene and propene in acid zeolite catalysis to produce active catalytic sites for MTO conversion. *J. Catal.* **2010**, *271*, 67−78.
(49) Sotelo-Boyás, R.; Froment, G. F. Fundamental Kinetic Modeling of Catalytic Reforming. *Ind. Eng. Chem. Res.* **2009**, *48*, 1107−1119.
(50) Davis, B. H. Alkane dehydrocyclization mechanism. *Catal. Today* **1999**, *53*, 443−516.
(51) Zhang, M.; Xu, S.; Wei, Y.; Li, J.; Chen, J.; Wang, J.; Zhang, W.; Gao, S.; Li, X.; Wang, C.; Liu, Z. Methanol conversion on ZSM-22, ZSM-35 and ZSM-5 zeolites: effects of 10-membered ring zeolite structures on methylcyclopentenyl cations and dual cycle mechanism. *RSC Adv.* **2016**, *6*, 95855−95864.
(52) Pan, L.; Xie, J.; Nie, G.; Li, Z.; Zhang, X.; Zou, J.-J. Zeolite catalytic synthesis of high-performance jet-fuel-range spiro-fuel by one-pot Mannich−Diels−Alder reaction. *AIChE J.* **2020**, *66*, No. e16789.
(53) Settle, A. E.; Berstis, L.; Rorrer, N. A.; Roman-Leshkóv, Y.; Beckham, G. T.; Richards, R. M.; Vardon, D. R. Heterogeneous Diels−Alder catalysis for biomass-derived aromatic compounds. *Green Chem.* **2017**, *19*, 3468−3492.
(54) Luo, M.; Wang, D.; Hu, B.; Fu, Y.; Mao, G.; Wang, B. The molecular structure and morphology of insoluble coke in SAPO-34 catalyst. *ChemistrySelect* **2017**, *2*, 5458−5462.

https://doi.org/10.1021/acsomega.1c05336
ACS Omega 2022, 7, 3277−3283